Supporting Information

Bioprosthesis of Core-Shell Gold Nanorod-Serum Albumin Nanoimitation: A Half-Native and Half-Artificial Nanohybrid for Cancer Theranostics

Hsien-Ting Chiu, Chung-Hao Chen, Meng-Lin Li, Cheng-Kuan Su, Yuh-Chang Sun, Chi-Shiun Chiang, and Yu-Fen Huang[*]

Prof. Yu-Fen Huang

Department of Biomedical Engineering and Environmental Sciences, National Tsing Hua University, Hsinchu 30013, Taiwan, ROC

Email: yufen@mx.nthu.edu.tw, Fax: (+ 886) 3-571-5131#34212

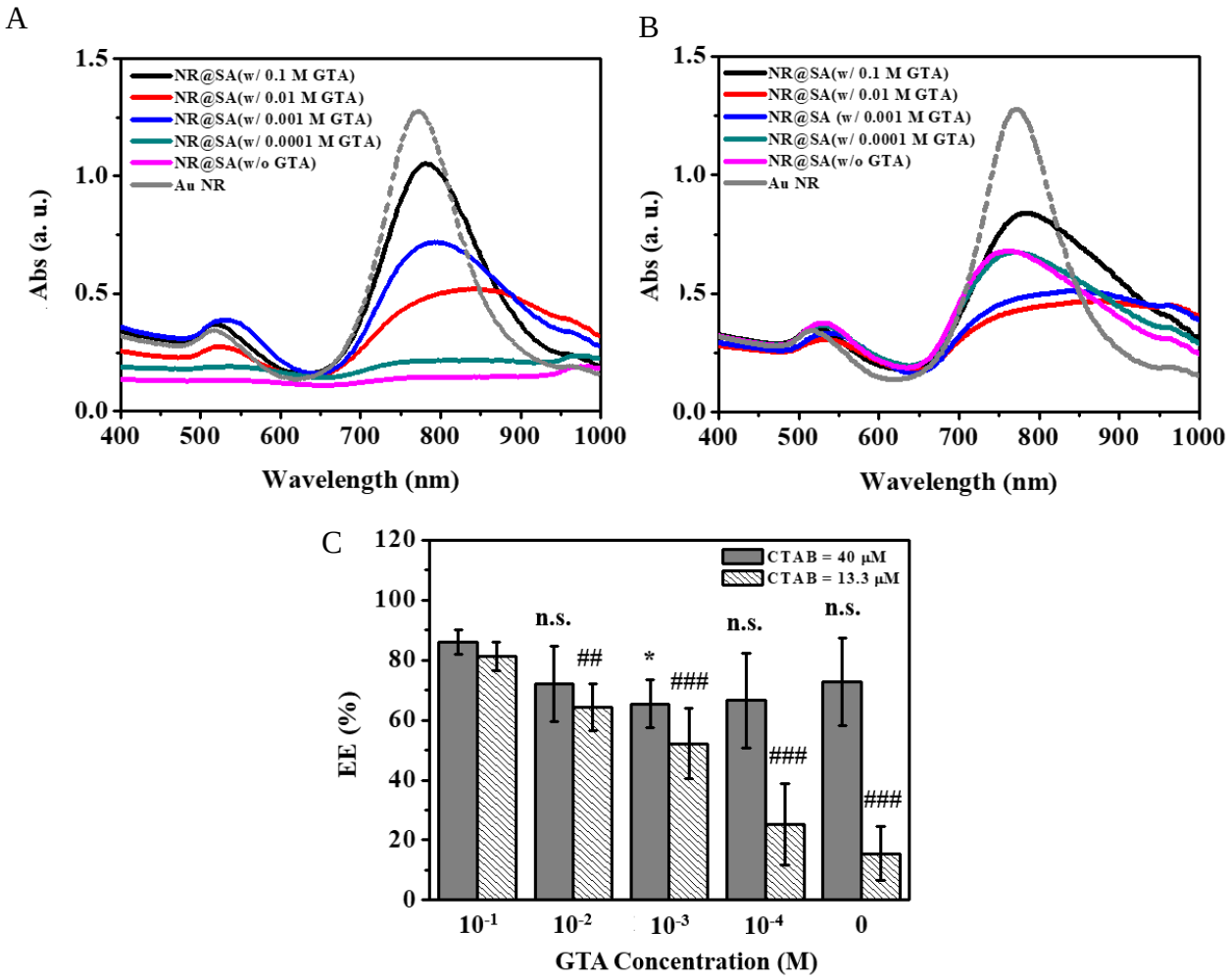

Figure S1. Preparation of NR@SA (GTA). UV-vis spectra of NR@SAs fabricated from a mixture of SA (3 μM), CTAB-capped Au NRs (0.6 nM), and serial concentrations of GTA (0–0.1 M). The CTAB concentration of the Au NR suspensions was (A) 40 μM and (B) 13.3 μM. To study the SA encapsulation efficiency of NR@SA, SA was functionalized with fluorescamine prior to fabrication of NR@SA. 5 mg/mL SA solution was reacted with 1.52 mM flourescamine in 1 × DPBS for 12 h under gently stirring. The resultant SA-FA was purified (7500 rpm, 10 min) by 10 k centrifugal filter to remove unlabeled fluorescamine. (C) The loading capacity of SA onto Au NRs was evaluated under different GTA concentrations. Fluorescamine-labeled SA was used for quantitative fluorescence analysis (excitation/emission: 390/470 nm). n = 4–5, *p < 0.05 or ns. p > 0.05, versus the use of 40 μM CTAB under 0.1 M GTA incubation; ##p < 0.01, ###p < 0.001, versus the use of 13.3 μM CTAB under 0.1 M GTA incubation.

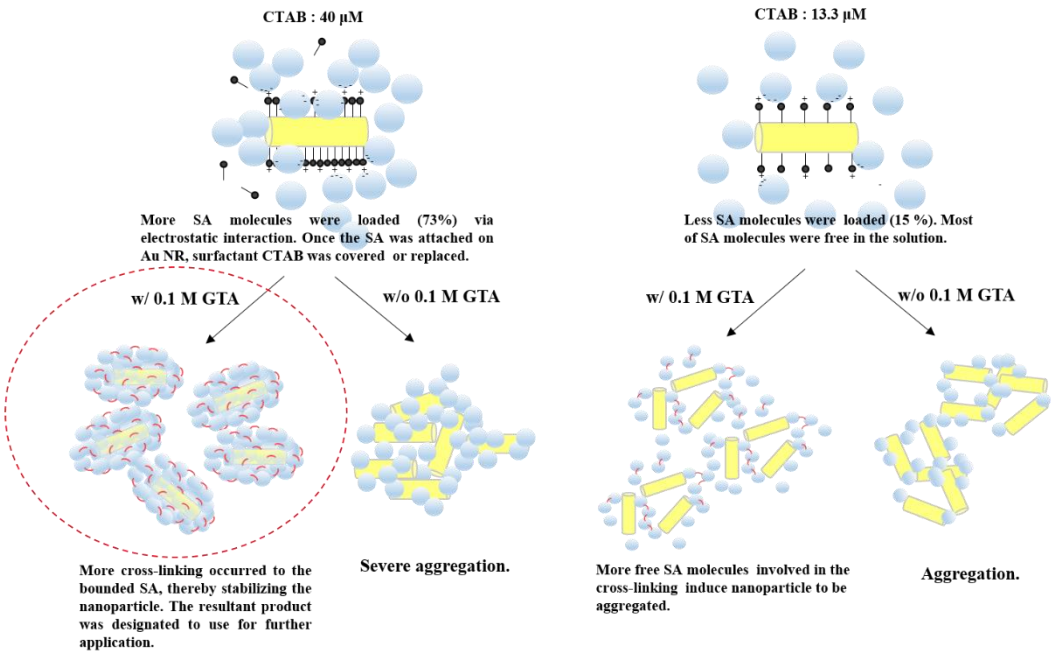

Figure S2. Schematic drawing demonstrating the effect of CTAB and GTA on SA cross-linking, and the resultant colloidal stability during the fabrication of NR@SAs.

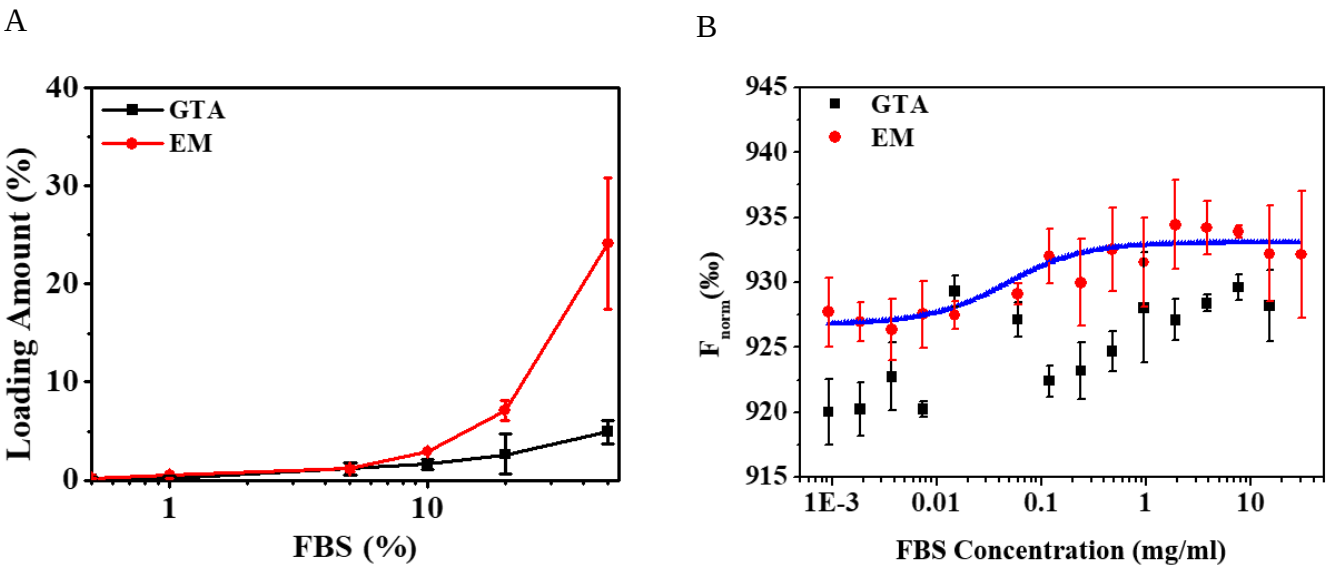

Figure S3. External serum protein (FBS) adsorption of NR@SAs (GTA) and NR@SAs (EM). To quantitatively analyze the protein adsorption onto different surface chemistry of SA shell, 100% FBS that equivalent to approximately 60 mg/ml protein was labeled with Cy5.5 and purified prior to further experiments. (A) 100% Cy5.5-labeled FBS diluted with DMEM (without phenol red) to a series concentrations of protein solution and then incubated with 2.4 nM NR@SA (GTA) or NR@SA (EM) for 6 h. The supernatants by fluorescence analysis were used to determine the loading amount of FBS on nanoparticles. (B) 2.4 nM NR@SA (GTA) or NR@SA (EM) incubated with a series dilution of FBS was analyzed through microscale thermophoresis. The volume ratio for the reaction of protein adsorption was 1:1 (v/v), and the final concentration of nanoparticles were all controlled in 1.2 nM. The blue line was represented the fitted curve of NR@SA (EM) whose K_D value was 48.6 ± 0.4 μg/ml whereas NR@SA (GTA) showed only nonspecific interaction with FBS protein. Compared to the K_D value for NR@SA (EM) and the corresponding loading amount of FBS (particularly high concentration of FBS), the results indicated that there should be different kinds of proteins in FBS which exhibits different and determined interactions with NR@SA (EM). Because the adsorbed protein on NR@SAs (EM) according to DLS profile in Figure 2B is highly presented as multilayers, we expect one or few proteins specific binding with nanoparticles that strongly determined the K_D value, and these adsorbed proteins are expected to be located in the inner layer of resultant protein corona. Other proteins in the outside layer of protein corona are nonspecifically interacted with the inner layer of protein corona.

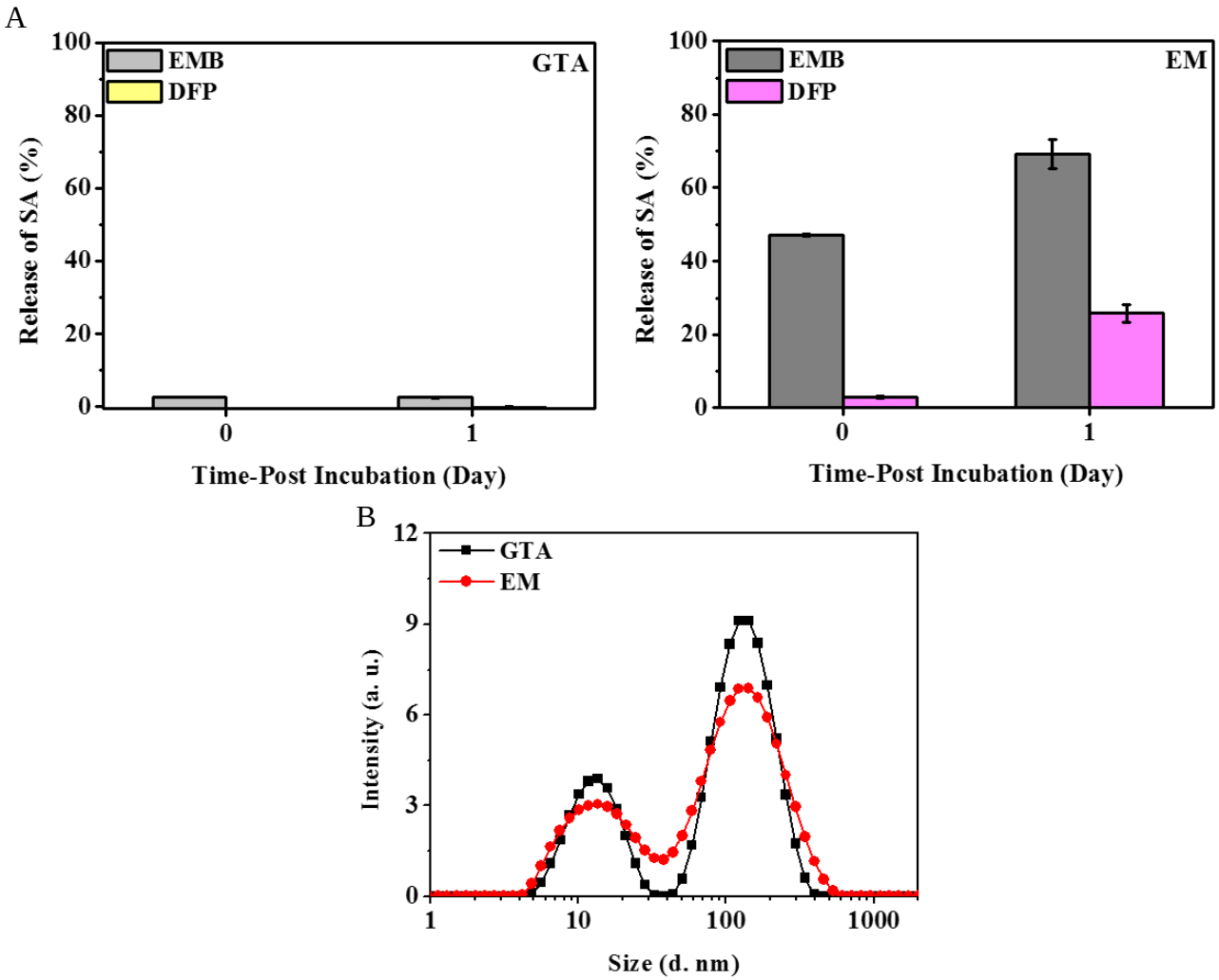

Figure S4. The colloidal stability of NR@SA. (A) Protein replacement of TRITC-labeled SA shell of 2.4 nM NR@SAs in endosomal mimicking buffer (EMB) and DFP (culture medium DMEM plus 10% FBS and 1% PS) after 0 h and 24 h incubation. EMB was served as positive control because amino acid, cysteine in the buffer was known to be able to replace the constructed shell of nanoparticles. 0 h referred to nanoparticles that were immersed with the designated buffer and vortex for 30 seconds, and then immediately centrifuged. The supernatants were collected and analyzed through fluorescence spectroscopy. EMB: 19.7 mL of 200 mM citric acid and 68.3 mL of 200 mM dibasic sodium phosphate with 190 mg L-cysteine. (B) The hydrodynamic size of NR@SA (GTA) and NR@SA (EM) after 24 h incubation with DFP.

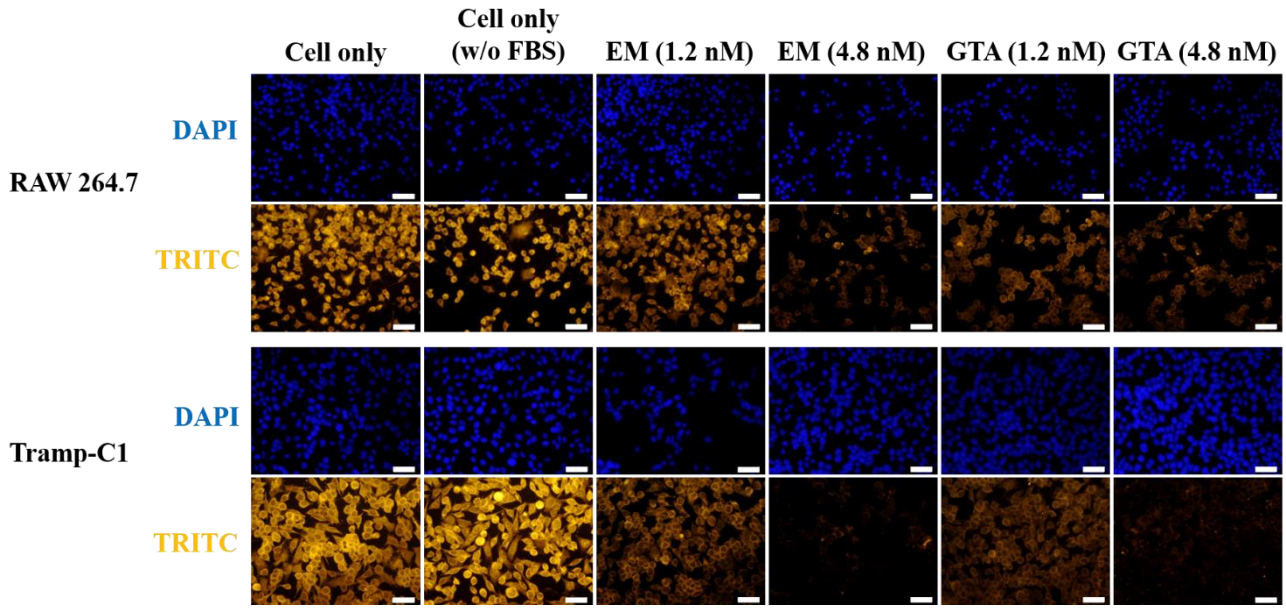

Figure S5. Competition test of NR@SAs with free SA. 15000 cells per well were incubated with DMEM (10% FBS) suspended NR@SAs (GTA) or NR@SAs (EM) for 6 h. In the middle of the incubation after 3 h, TRITC-labeled SA (2 wt%) was spiked in the solution and started the competition test with NR@SAs. The final concentration of TRITC-labeled SA was 3 μM whereas both nanoparticles concentration were maintained in 1.2 nM or 4.8 nM which 0.6 nM nanoparticles was respected with 2.7 μM SA. After incubation (6 h for nanoparticles and 3 h for TRITC-labeled SA), cells were washed with DPBS twice and fixed in 4 % PFA before microscopy observation. Scale bar: 50 μm.

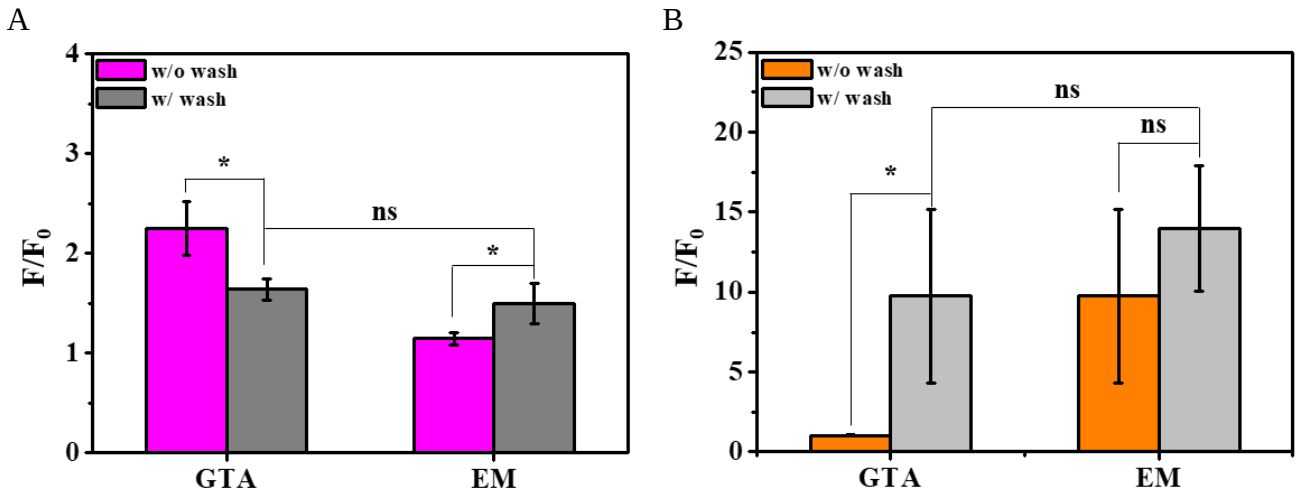

Figure S6. Surface functional group of different constructed SA shell. (A) Carboxyl group and (B) amine group of constructed SA shell was determined by 5-aminofluorescein and fluorescamine, respectively. 1.2 nM nanoparticles are either washed with DI water one time (w/o SA wash) or washed with 1 wt% SA two times and 0.1 wt% SA one time (w/ SA wash). The final concentration of free SA was controlled less than 0.002 wt% SA which was approximately 5.6% of the concentration of the constructed SA shell. The as-prepared nanoparticles were first incubated with 80 μM and 20 μM of fluorescamine and 5-aminofluorescein for 1 h. Then they were centrifuged (5500 g, 15 min) and re-suspended in DI water. This procedure was repeated twice. To remove unbounded or weakly-bounded proteins, 98% of supernatant was removed from each centrifugation. Dye-labeled SA of NR@SAs was surprisingly stable during centrifugation without any aid of free protein. Dye fluorescence was analyzed through fluorescence spectroscopy. $n = 3$, $*p < 0.05$ or ns. $p > 0.05$.

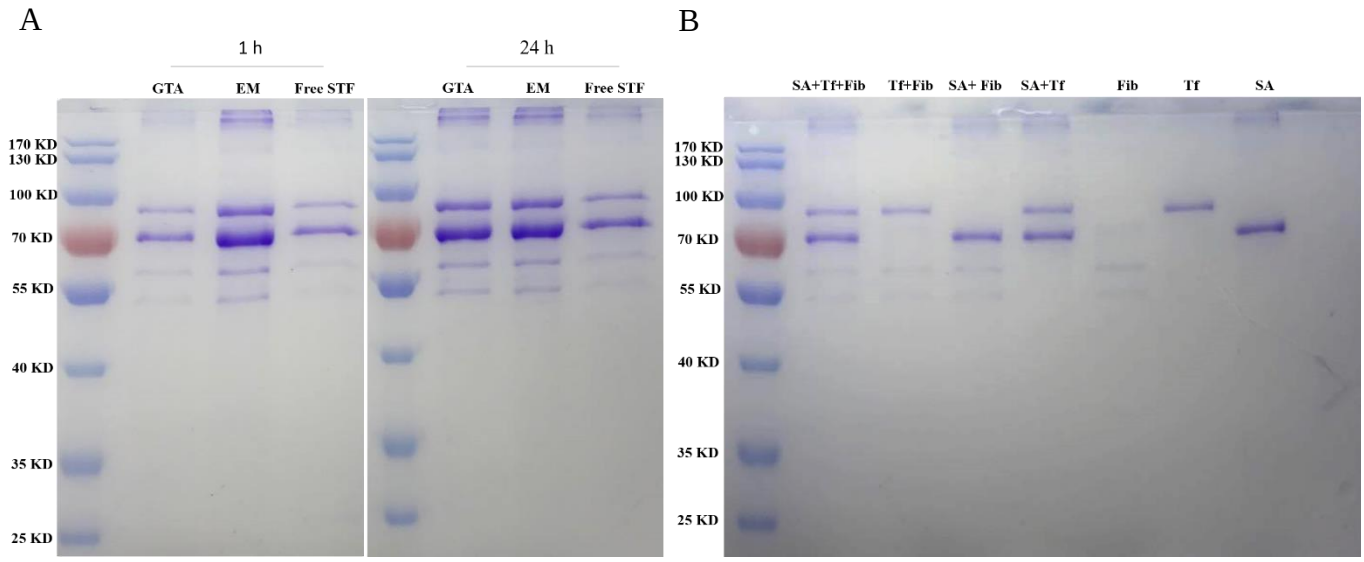

Figure S7. SDS-PAGE gel analysis of protein adsorption. (A) 1.2 nM nanoparticles after incubation with STF protein solution (STF = SA: 151.5 μM (1 wt%) + Tf : 37.5 μM + Fib: 13.2 μM in PBS) for 1 h or 24 h was first diluted with PBS to 0.24 nM and centrifuged (5500 g, 15 min) to remove most unbounded proteins. The free protein should remain only 0.5% of original STF solution. The solution was then diluted to 6-fold reduction and together with STF protein solution (150-fold dilution) for gel analysis. (B) To identify the markers form each protein, free protein solution that contained SA (1 wt%), Tf (37.5 μM) and Fib (13.2 μM) individually or the mixture of two or all kinds of protein was diluted to 150-fold decrease for gel analysis.

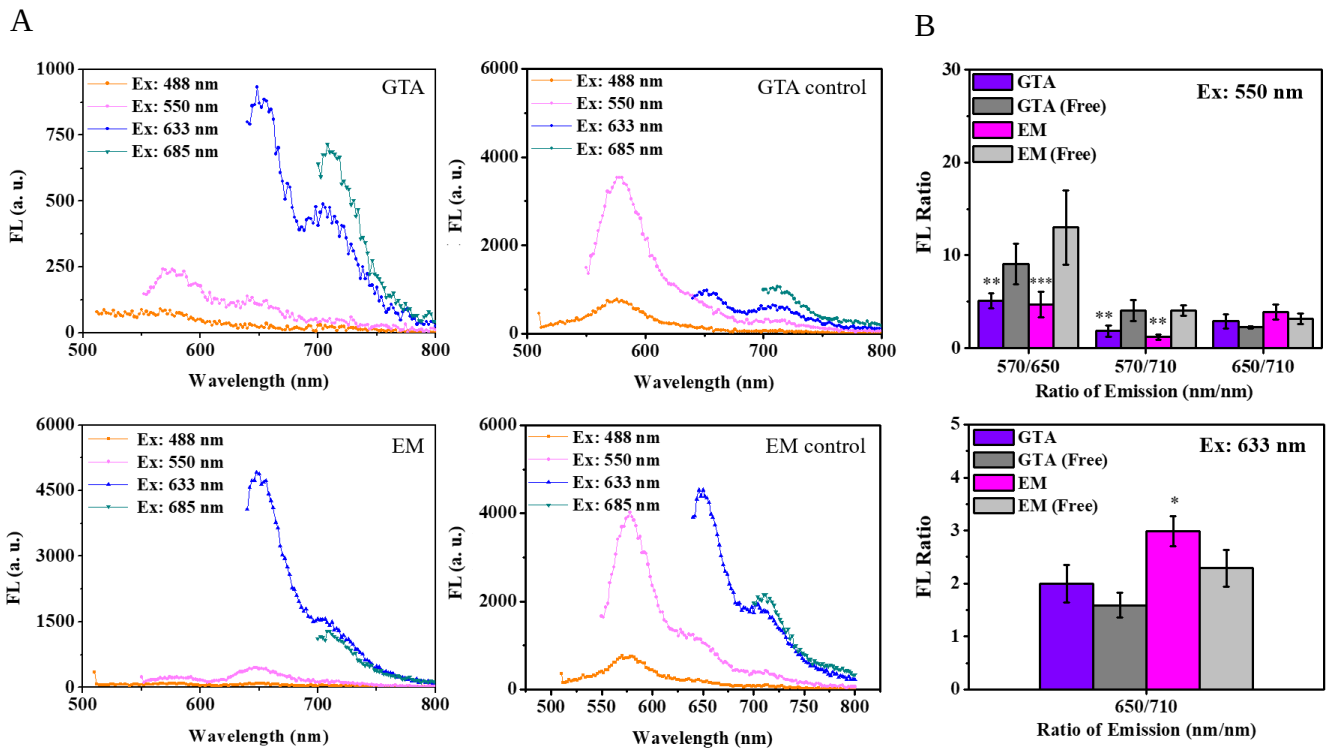

Figure S8. (A) Monitoring the mechanism of protein adsorption by fluorescence resonance energy transfer (FRET). Similar to Figure 5A and Figure 5B, the procedure was exactly the same, except Fib was equipped with Cy5.5 rather than Alexa-488. 10 % (1.3 μM) of Cy 5.5-modified Fib was replaced with native Fib in STF solution. (B) The change of energy transfer was presented as a fluorescent ratio of emission. $n = 3$, $^{*}p < 0.05$, $^{**}p < 0.01$ or $^{***}p < 0.001$.

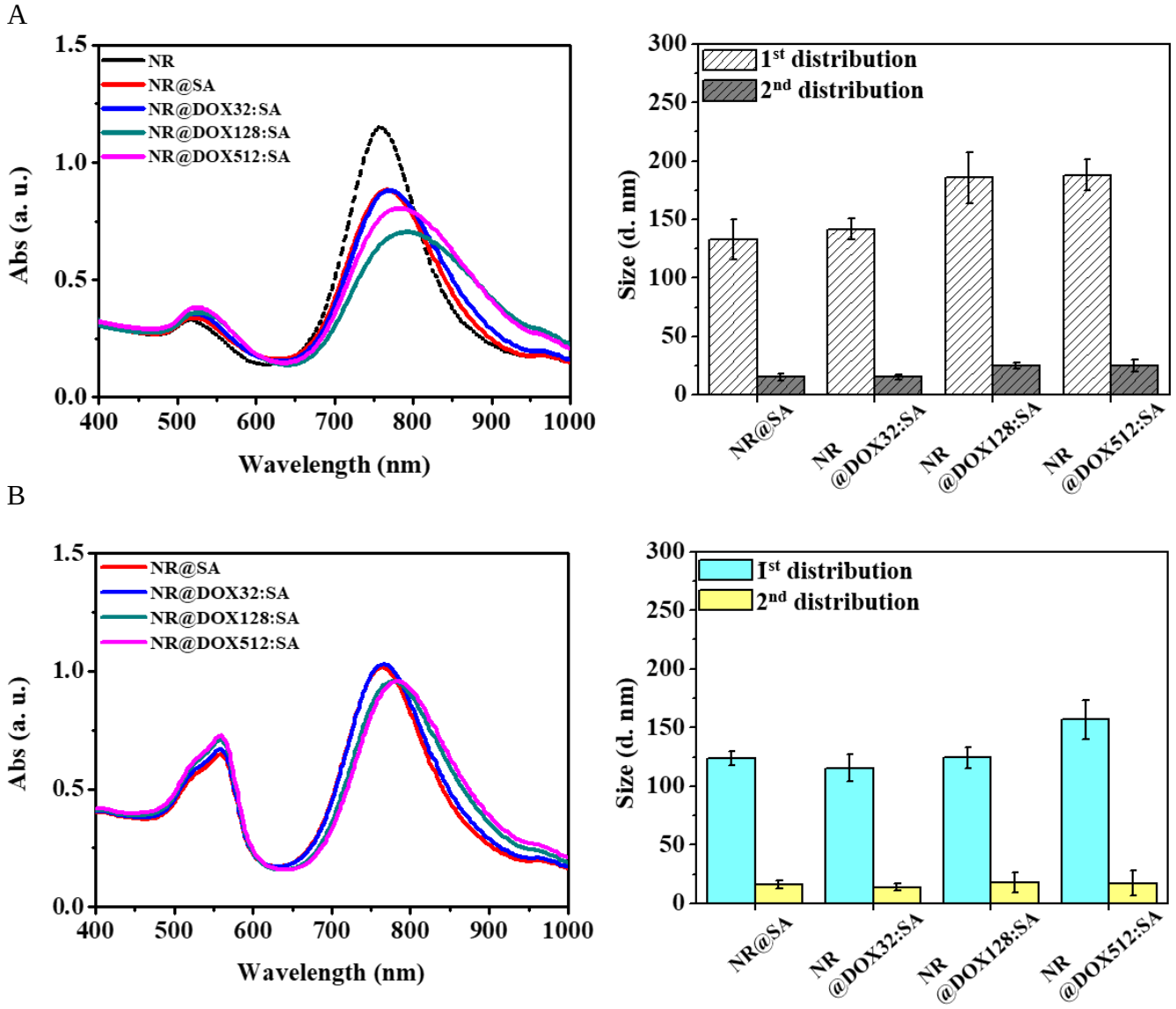

Figure S9. UV-vis spectra and hydrodynamic size of NR@SAs and NR@DOX:SAs in (A) PBS and (B) DFP. Labels 1st and 2nd in the figure indicated the two distributions of DLS profile of NR@SAs (GTA) that are defined in Figure 2B. *n* = 3.

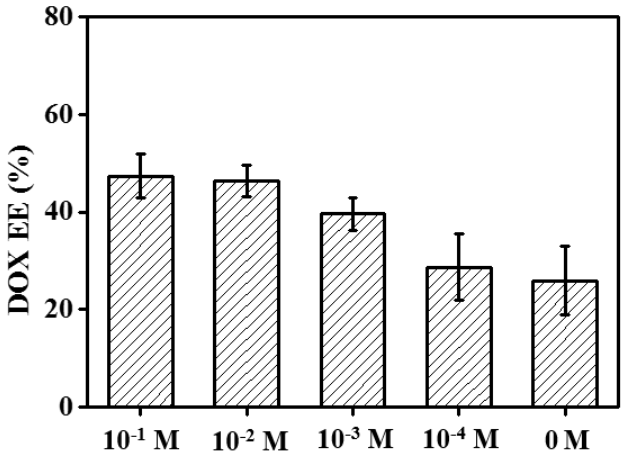

Figure S10. Effect of various GTA concentrations (0–0.1 M) on the drug encapsulation efficiency of NR@DOX:SA (Au NR: 0.6 nM, DOX: 9.4 μM) fabrication.

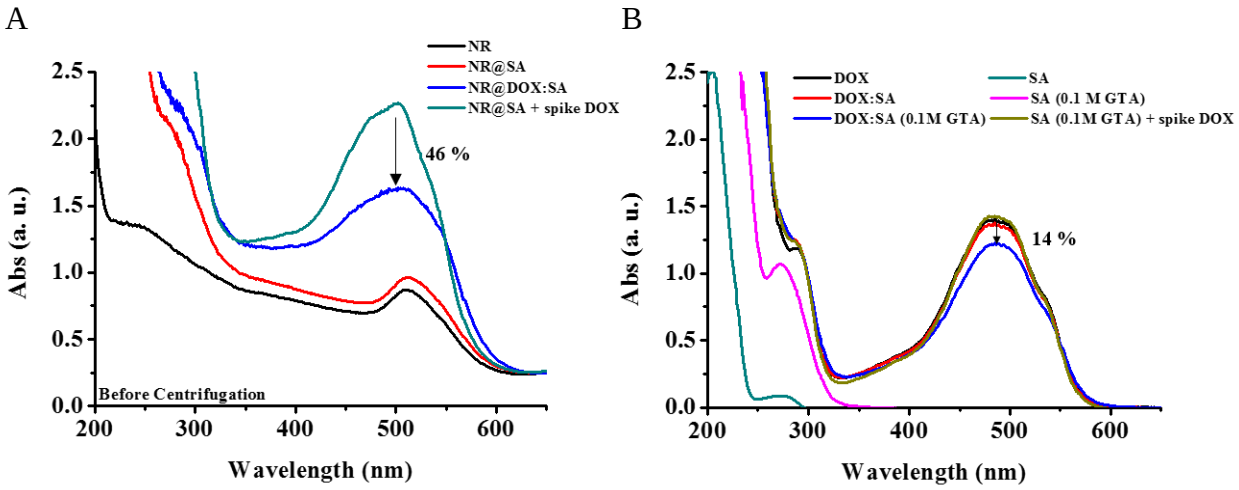

Figure S11. The (A) presence and (B) inexistence of Au NR in the cross-linked SA matrix exhibited a greater significant decrease in the absorption intensity of DOX at 490 nm. The Au NR and DOX concentration of all samples was maintained at 0.6 nM and 55.8 μM, respectively.

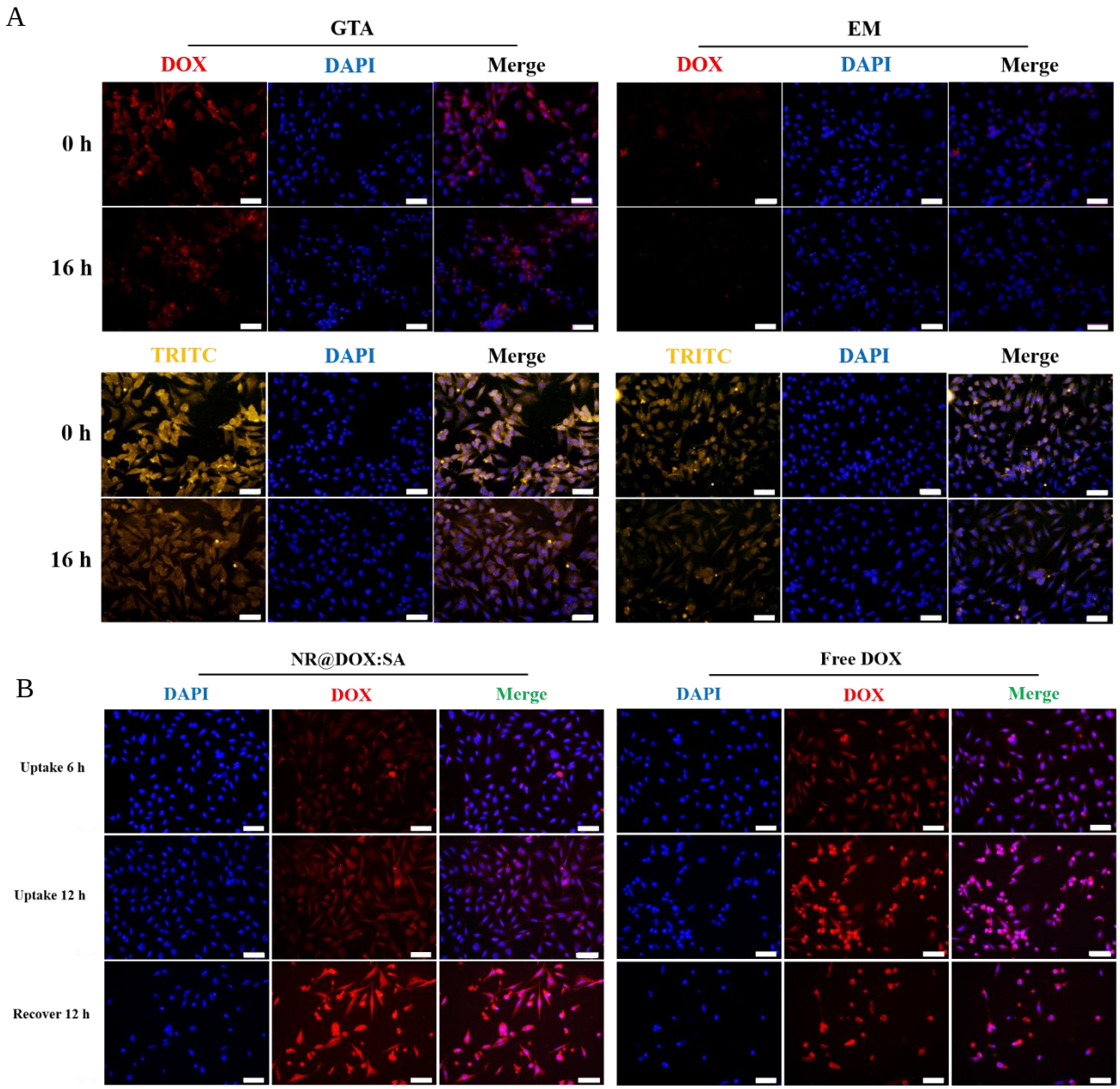

Figure S12. NR@SA nanoplatform for intracellular payloads delivery. (A) 1.2 nM of NR@DOX:SAs (GTA), NR@DOX:SAs (EM), NR@SA-TRITC (GTA) or NR@SA-TRITC (EM) were incubated with Tramp-C1 cells for 6 h and recovered with fresh medium for 0 and 16 h. DOX and TRITC fluorescence was monitored by fluorescence microscopy. DOX concentration of NR@DOX:SAs (GTA) and NR@DOX:SAs (EM) with respect to 0.6 nM Au NRs was 9.4 μM and 7.9 μM, respectively. Scale bar: 50 μm. (B) To clarify the fluorescence change between NR@DOX:SAs (GTA) and free DOX, 0.6 nM of NR@DOX:SAs (GTA) and corresponding free DOX uptake by Tramp-C1 cancer cells is adjusted and visualized at different time points using fluorescence microscopy. The Au NR with respect to DOX concentration for NR@DOX:SAs was maintained at 0.6 nM and 9.4 μM, respectively. Scale bar: 50 μm.

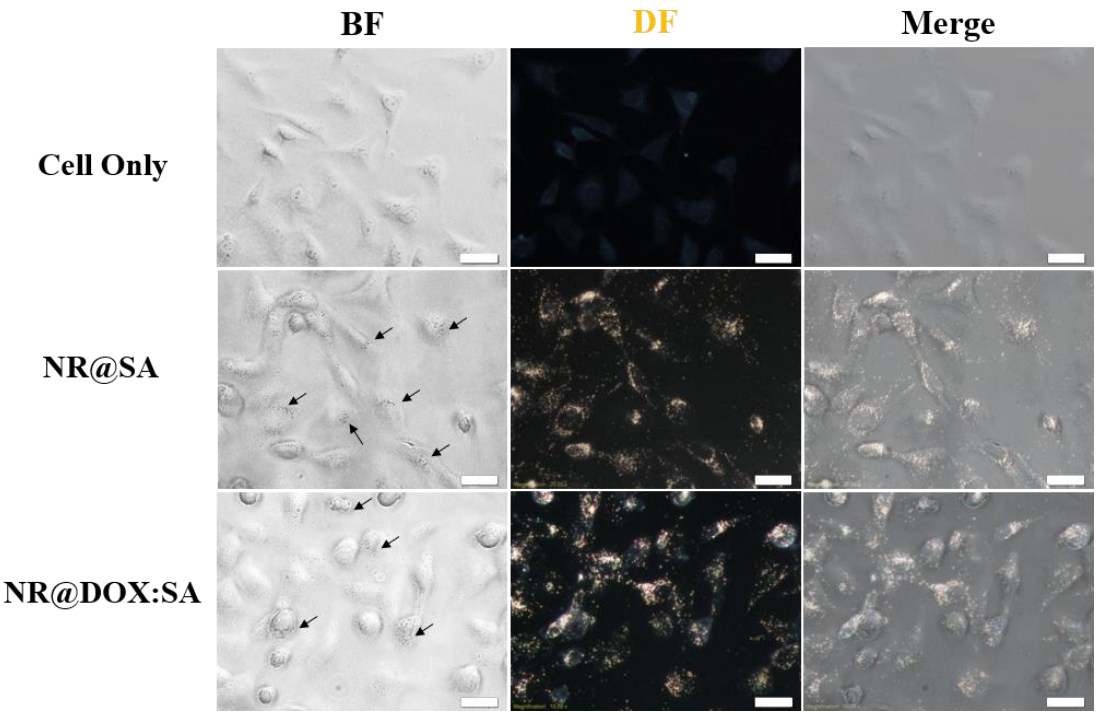

Figure S13. Dark-field microscopic images of the intracellular uptake of NR@SAs and NR@DOX:SAs by Tramp-C1 cells after 24 h. The Au NR and DOX concentration for all samples was maintained at 0.6 nM and 9.4 μM, respectively. Scale bar: 50 μm.

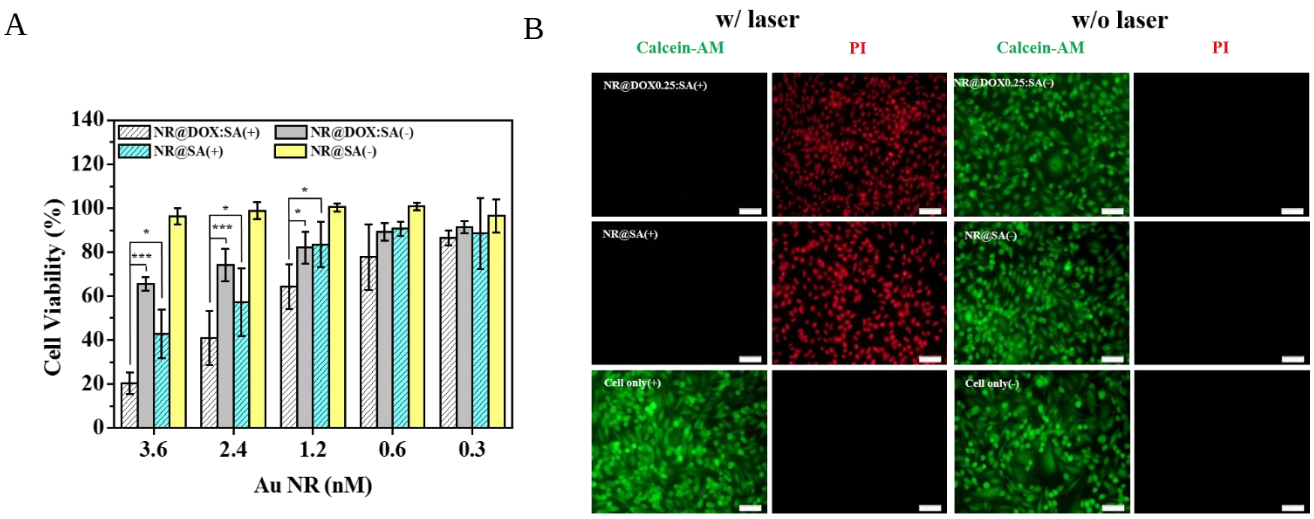

Figure S14. Photothermal effect for anti-cancer activity. (A) To assess the photothermal effect, cells were incubated with NR@SAs and NR@DOX0.25:SAs for 24 h, followed by NIR light irradiation (808 nm, 2.65 W/cm^2, 1 h). Cells were allowed to recover for an additional 48 h in fresh culture medium prior to the use of an AlamarBlue assay. n = 5, *p < 0.05, ***p < 0.001. (B) Live/dead cell double staining assay of Tramp-C1 cancer cells treated with NR@SAs and NR@DOX0.25:SAs followed by NIR irradiation (808 nm, 2.65 W/cm^2, 1 h). The Au NR and DOX concentration of all samples was maintained at 2.4 nM and 1 μM, respectively. Cells were stained with 1.5 μM calcein-AM (green) and 2.5 μM propidium iodide (PI, red) for 30 min before observation using fluorescence microscopy. Scale bar: 50 μm.

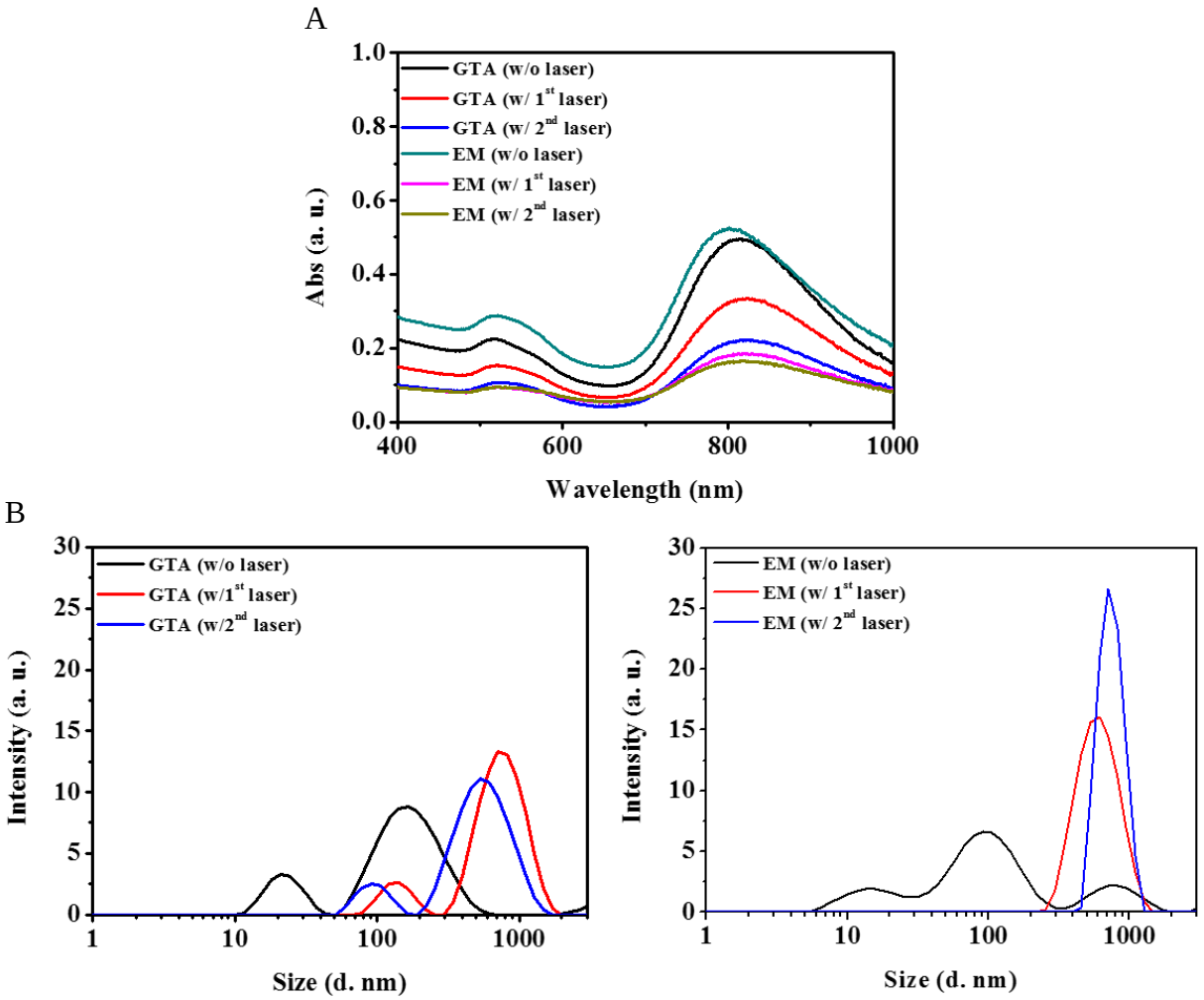

Figure S15. (A) UV-vis spectra and (B) hydrodynamic size of NR@SAs (GTA) and NR@SAs (EM) with or without NIR-laser irradiation in lysosomal-mimicking buffer (with 1.2 U/ml enzyme cathepsin B). 2.4 nM of nanoparticles in lysosomal-mimicking buffer was irradiated with either 0, 1 or 2 times of NIR-laser irradiation at 808 nm. Each treatment was 10 min at the power density in 2.65 W/cm^2. After NIR-laser irradiation, nanoparticles were diluted to 0.3 nM with lysosomal-mimicking buffer before further analysis. Notably, the size profiles of both nanoparticles that are exposed with 1 or 2 times of NIR laser with large deviation were no significant difference between each other.

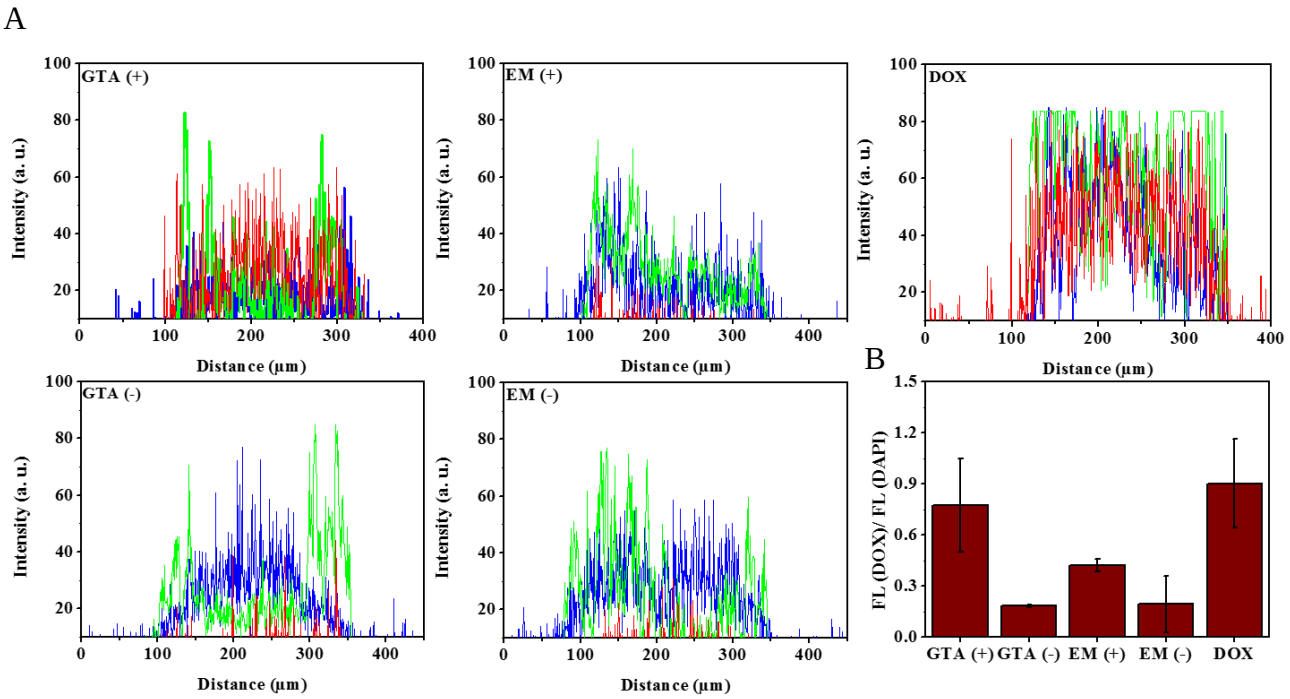

Figure S16. Quantitative analysis of confocal microscopic images. (A) Each fluorescent channel of DAPI, calcein-AM and DOX was analyzed alone with x-axis (Figure 7D, white dash line, x direction). (B) The fluorescence intensity of 4–5 tumor spheroids from each group after quantitative analysis was obtained. DOX signal was normalized by dividing to the intensity of DAPI fluorescence for further comparison.

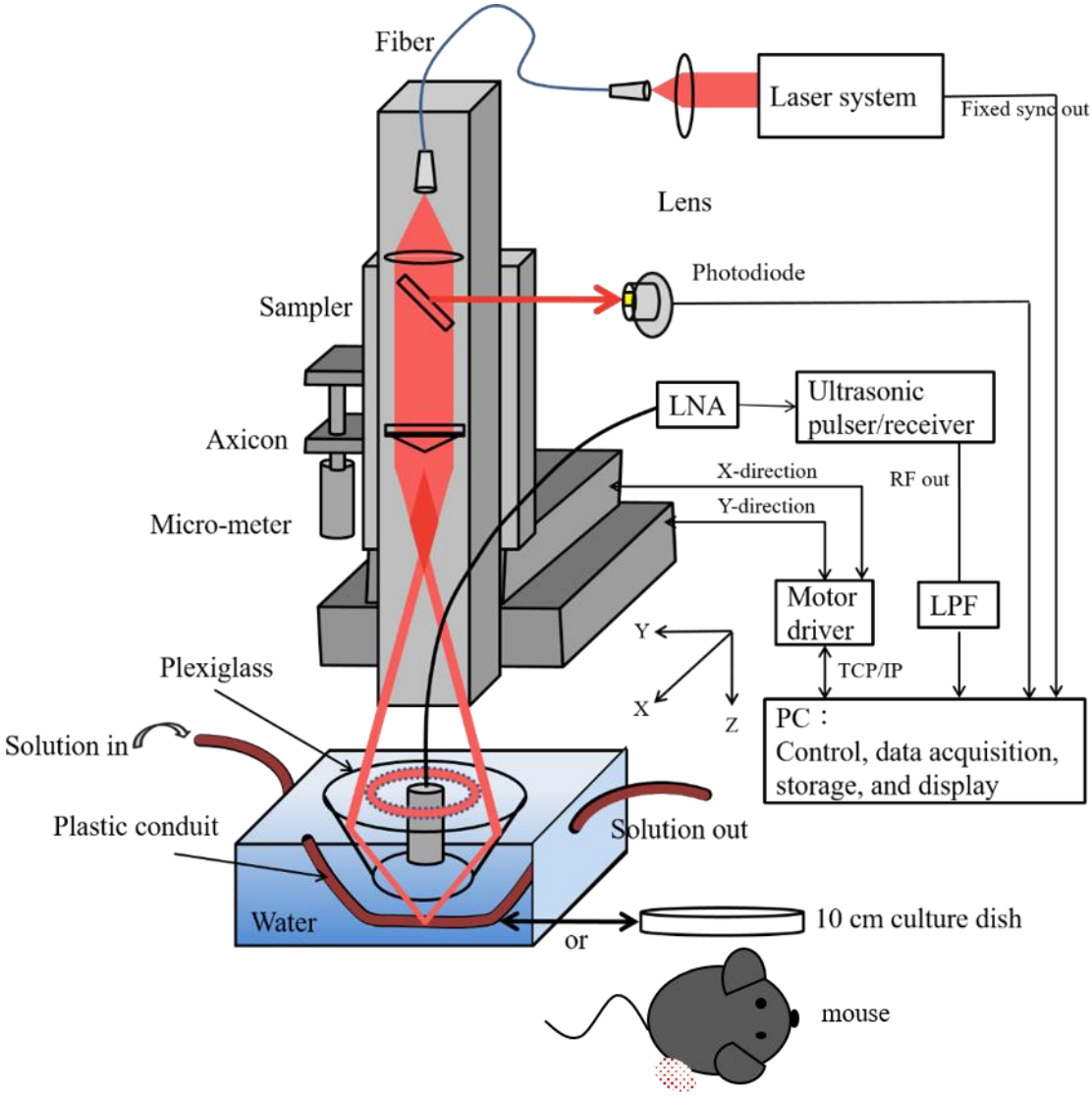

Figure S17. Schematic diagram of the photoacoustic system.

A

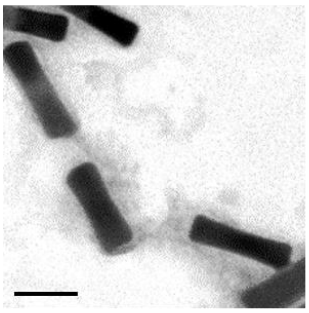

B

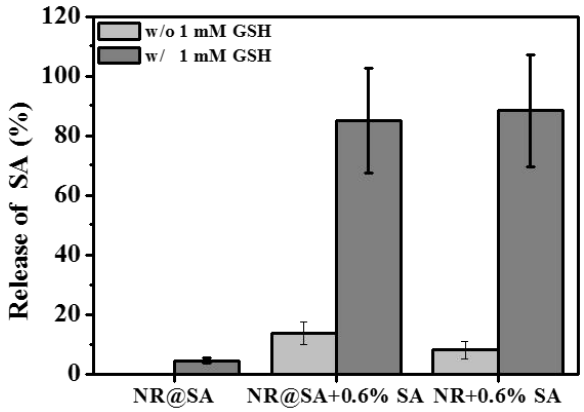

Figure S18. Hard and soft protein corona. (A) Negative staining TEM images of NR:SA. Scale bar: 50 nm. (B) An SA desorption study was performed separately on fluorescence-labeled NR@SAs, as well as NR@SAs and Au NRs pre-equilibrated with fluorescence-labeled SA (SA-TRITC) of 0.6 wt%. Three different nanoconjugates were denoted as NR@SA-TRITC, NR@SA:SA-TRITC, and NR:SA-TRITC. An individual suspension was subsequently in contact with 1 mM glutathione (GSH) for 24 h to replace the fluorescence labeled SA.

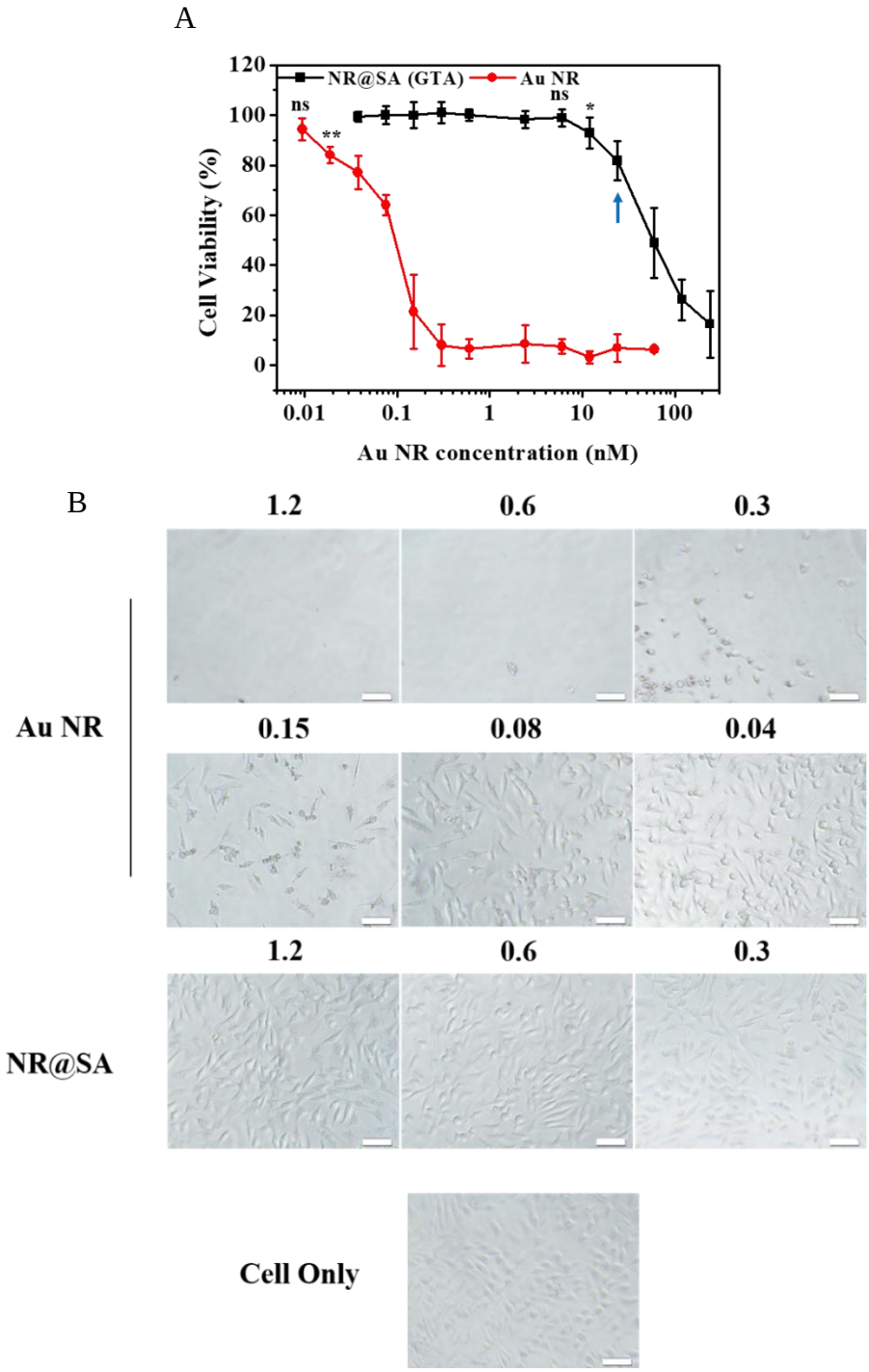

Figure S19. Cytotoxicity of Au NRs and NR@SAs treated Tramp-C1 cells. (A) NR@SAs (GTA) and pure Au NRs with a series of concentrations was prepared in DMEM (with 10% FBS) for 24 h incubation with Tramp-C1 cells. The cytotoxicity was assessed through an Alamarblue assay after 48 h cell recovery. The IC_{50} of NR@SA (GTA) and pure Au NR was 60.6 nM and 0.1 nM, respectively. The blue arrow indicated the concentration selected for *in vivo* experiments. The statistical analysis indicated the minimum toxic concentration of NR@SA (GTA) and pure Au NR. $n = 4$, $*p < 0.05$, $**p < 0.01$ or ns. $p >$

0.05, versus non-treated cells. (B) Microscopic images of Au NRs and NR@SAs treated Tramp-C1 cells. NR@SAs (GTA), and pure Au NRs ranged from 0.04 to 1.2 nM were incubated with cells for 24 h. Cells were fixed with 4% paraformaldehyde prior to observation by bright-field microscopy. Scale bar: 100 μm.

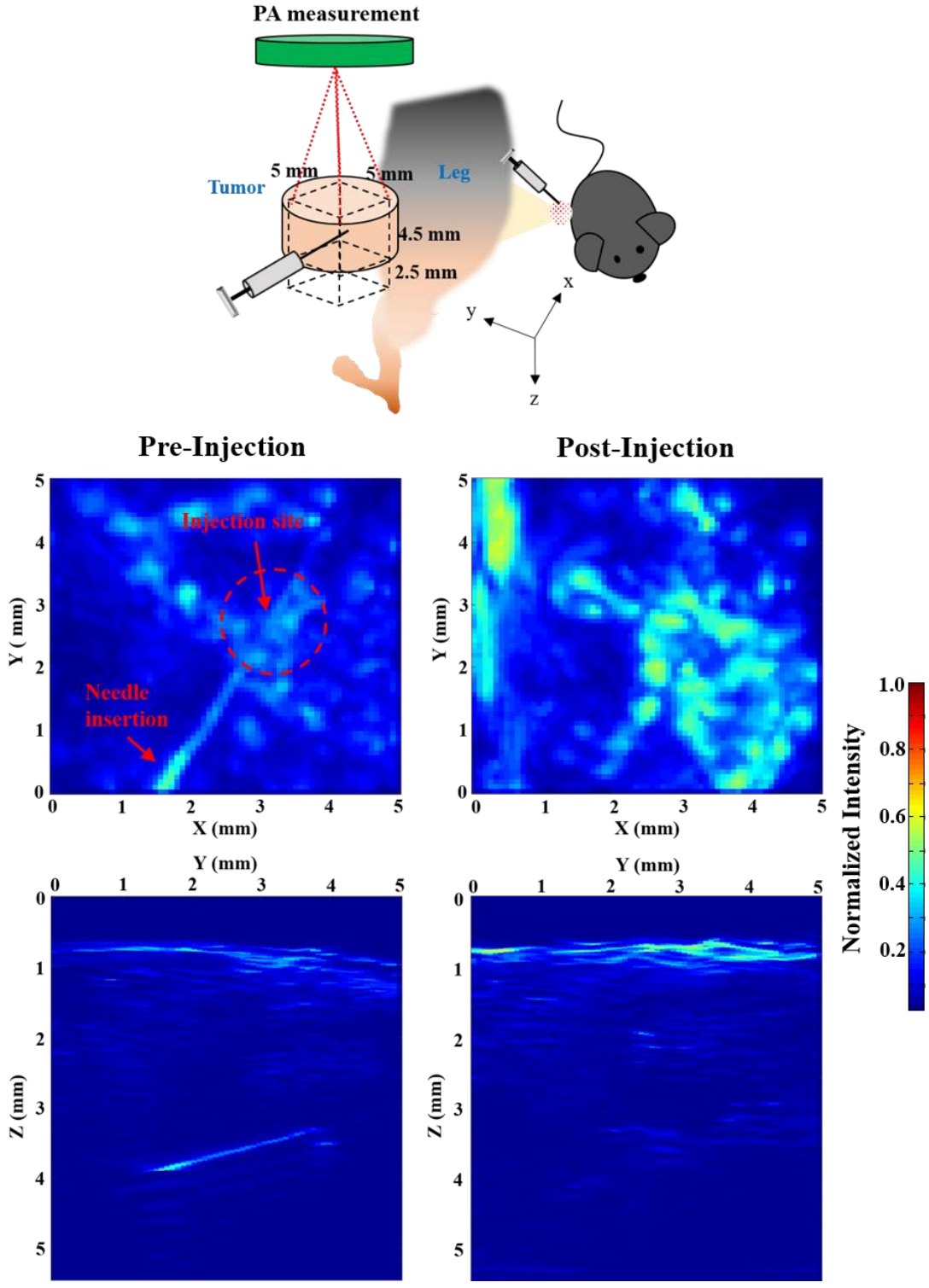

Figure S20. Capability of NR@SA nanoplatform for in vivo photoacoustic imaging. Maximum amplitude projection and PA B-mode images of the selected tumor volume was acquired from tumor-bearing mice during, and after local delivery of NR@SAs.

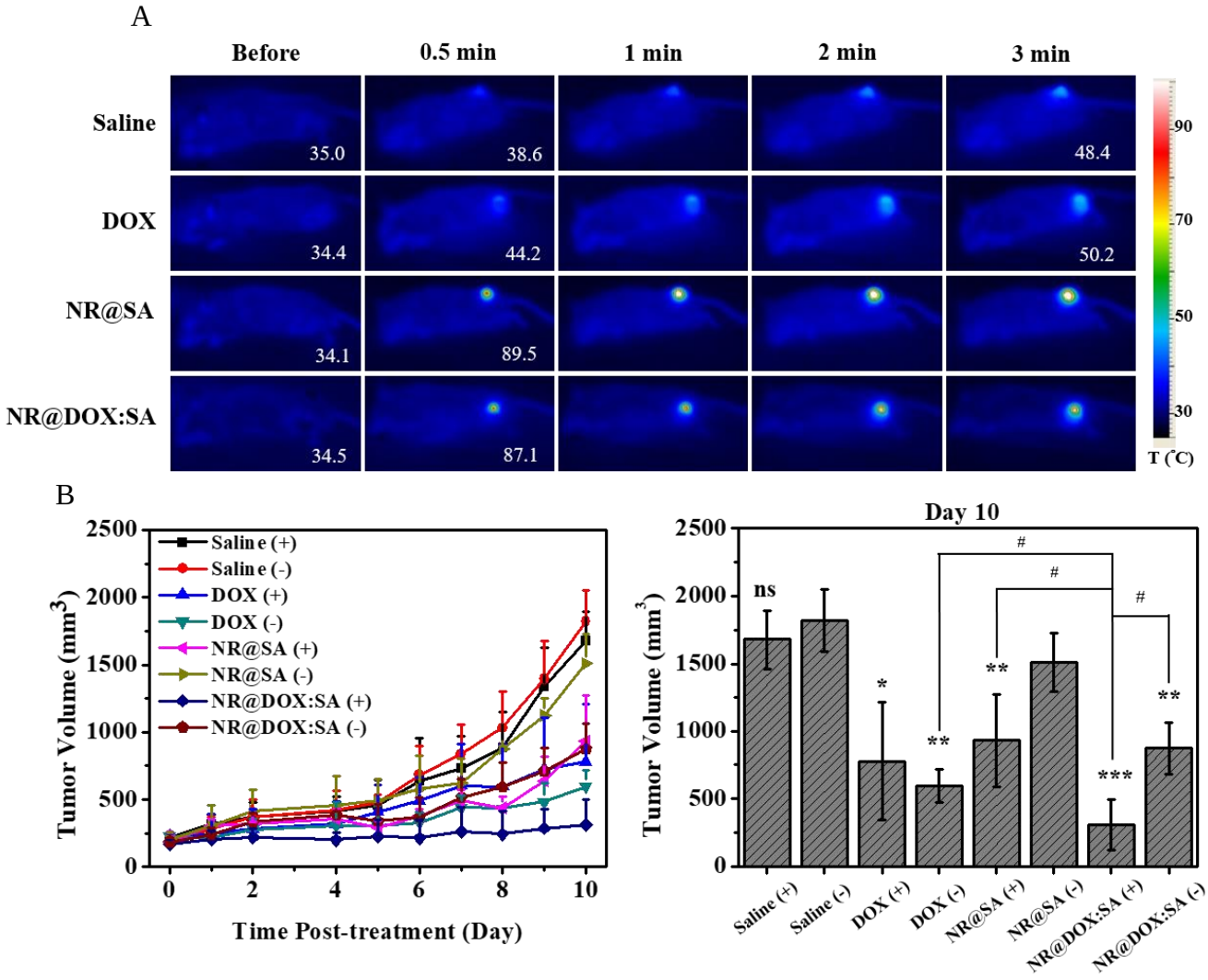

Figure S21. Capability of NR@SA nanoplatform for in vivo cancer therapy. 2×10^6 Tramp-C1 cells were subcutaneously injected into both the left and right hind limbs of the 6 to 8 week-old male C57BL/6J mice. When the tumor size reached 150 mm^3, mice were randomly divided into four groups (n = 3–5 per group). After intratumorally receiving 50 μL of different agents including PBS, DOX, NR@SAs, and NR@DOX:SAs, the tumor on the right limb was subjected to 3 mins of NIR laser irradiation (808 nm, 2.65 W/cm^2) at 24 h post-dosing. (A) Real-time thermal images were captured to monitor the temperature rise of treated tumors under light exposure. (B) Tumor growth curve and tumor volume on day 10 of mice receiving various treatments. Au: 3.36 mg/kg, DOX: 2.5 mg/kg. n = 3–5, $^{**}p < 0.01$, $^{***}p < 0.001$ or ns. $p > 0.05$, versus PBS (-). $\#p < 0.05$.

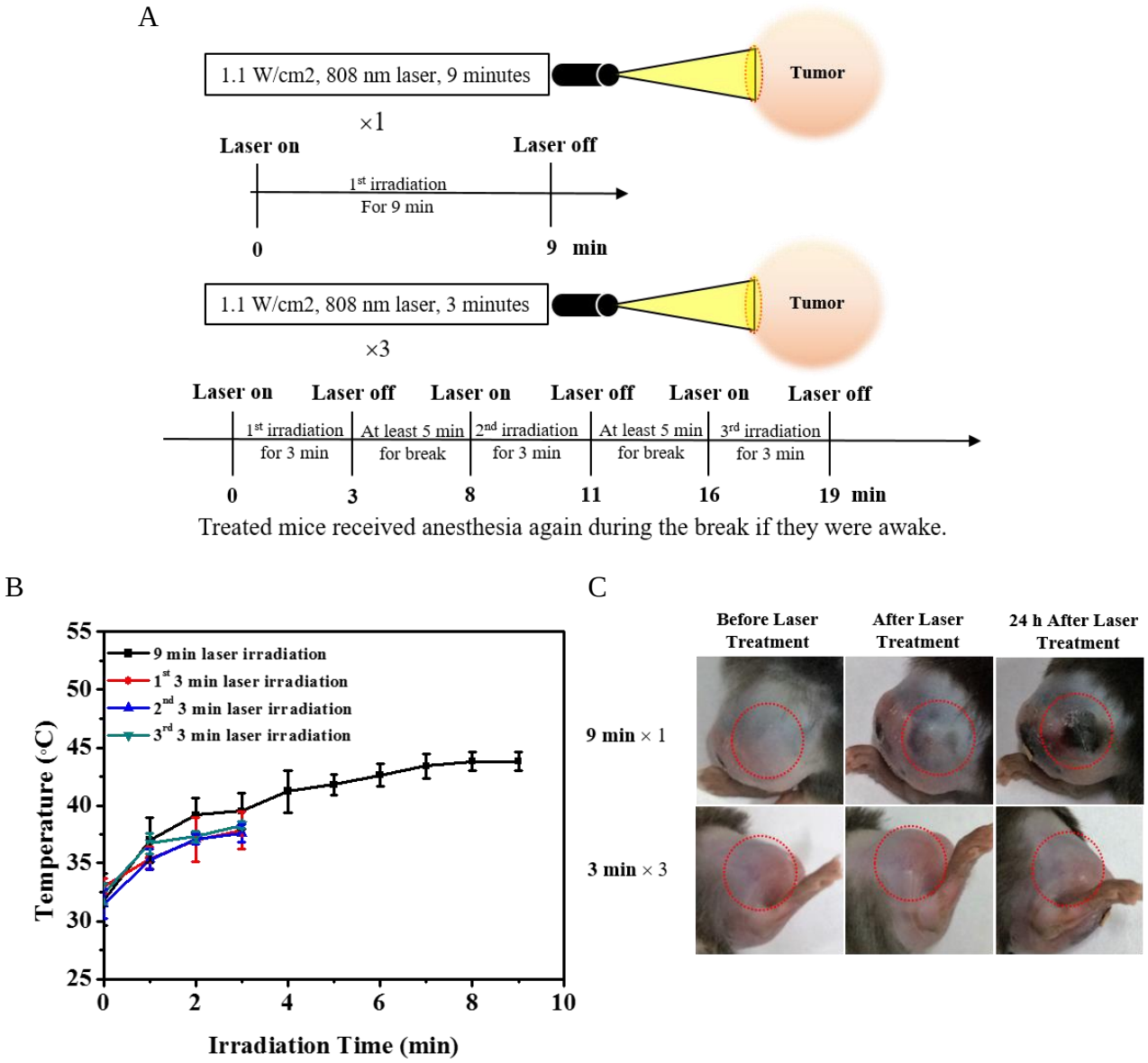

Figure S22. (A) Schematic illustration demonstrating the optimized strategy for photothermal treatment. When the tumor size of Tramp-C1 bearing mice reached 1.5 cm, non-treated tumors were subjected to either 3 min or 9 min (repeated 3 times) of NIR light irradiation at a power density of 1.1 W/cm^2. (B) The rises in temperature as well as (C) representative digital images of the tumor-bearing mice were recorded at selected time points during light exposure.

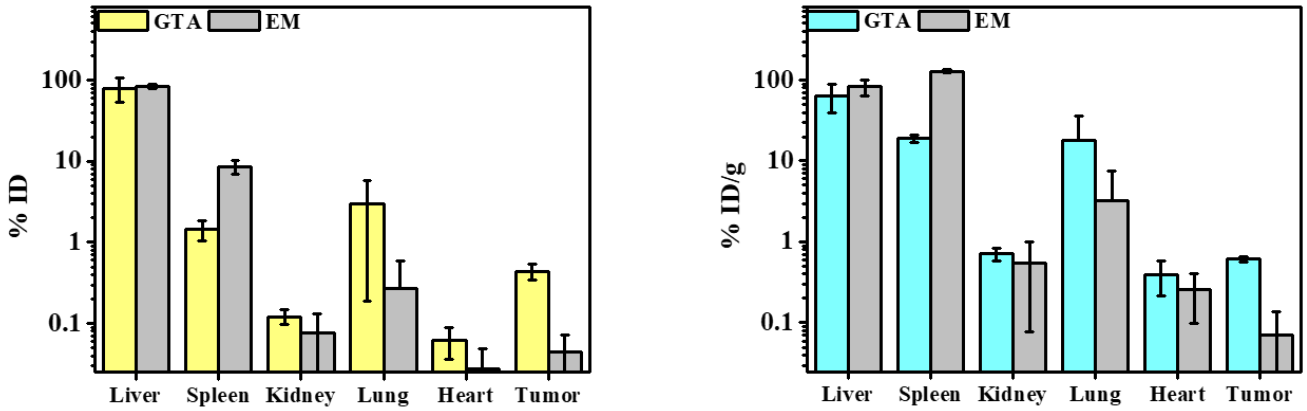

Figure S23. In vivo bio-distribution of NR@SAs. 0.65 mg/kg NR@SA (GTA) was intravenously administrated into three Tramp-C1 tumor-bearing mice when the tumor grew to approximately 150–250 mm^3. At 24 h post-injection, the mice were sacrificed and the major organs were immersed in aqua regia for ICP-MS analysis. Furthermore, two mice injected with NR@SA (EM) were served as the negative control. Based on the fact that NR@SAs (EM) showed limited tumor accumulation in Tram-C1 bearing mice in our previous study,[1] NR@SAs (EM) is delivered at a relatively high level (3.4 mg Au/kg) in the current regimen.

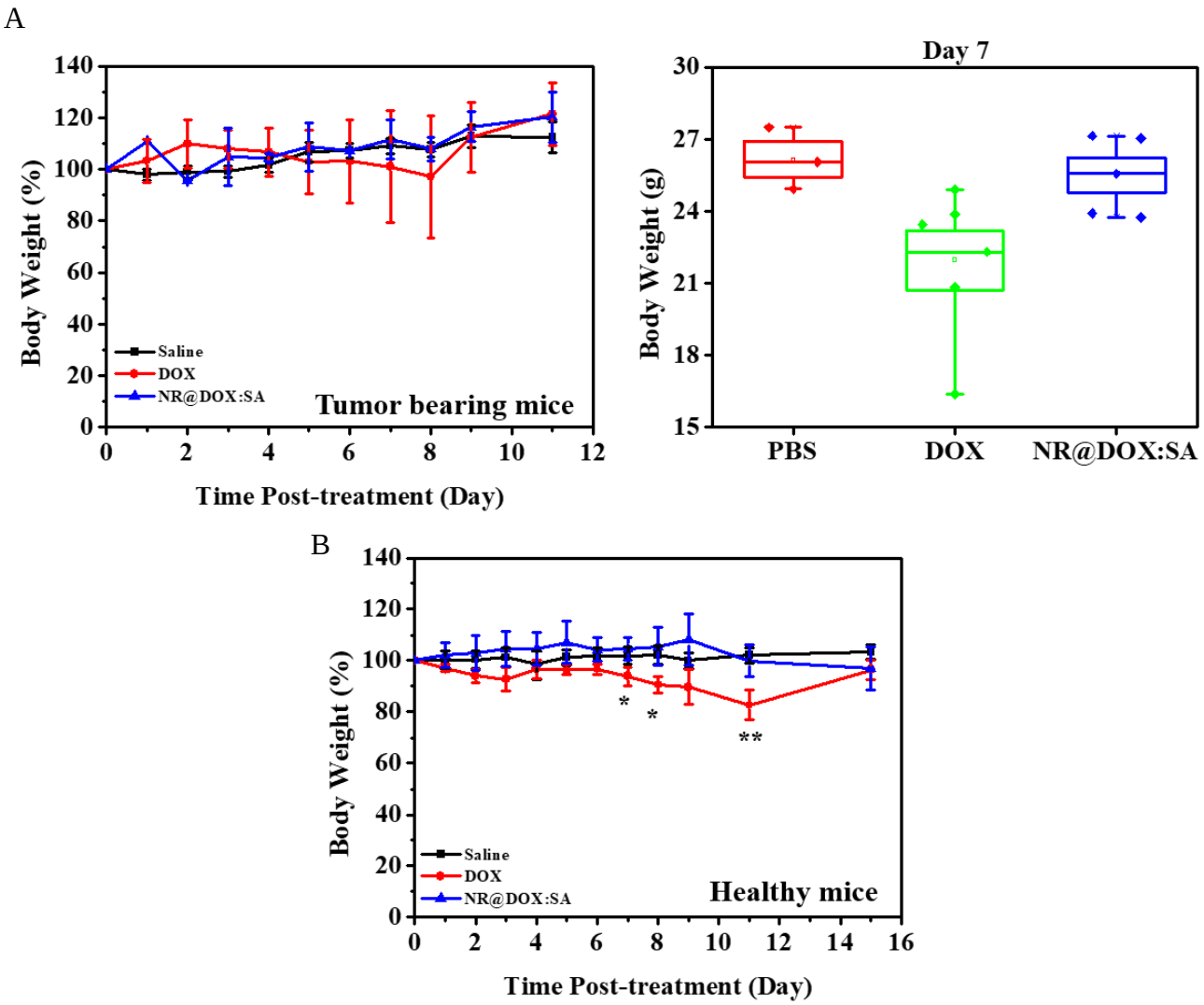

Figure S24. Body weight of (A) Tramp-C1 tumor bearing mice and (B) healthy mice after receiving different treatments including PBS, free DOX, and NR@DOX:SAs were collaterally measured. Au: 3.36 mg/kg, DOX: 15 mg/kg. n = 3–6, *p < 0.05, **p < 0.01 versus PBS-treated healthy mice.

Reference

1. Chiu, H. T.; Su, C. K.; Sun, Y. C.; Chiang, C. S.; Huang, Y. F., Albumin-Gold Nanorod Nanoplatform for Cell-Mediated Tumoritropic Delivery with Homogenous ChemoDrug Distribution and Enhanced Retention Ability. *Theranostics* **2017,** *7* (12), 3034-3052.